RESEARCH ARTICLE

Free Convection Boundary Layer Flow from a Vertical Truncated Cone in a Hybrid Nanofluid

Muhammad Khairul Anuar Mohamed[a,*], Anuar Ishak[b], Ioan Pop[c], Nurul Farahain Mohammad[d], Siti Khuzaimah Soid[e]

[a]Centre for Mathematical Sciences, College of Computing and Applied Sciences, Universiti Malaysia Pahang, 26300 UMP Kuantan, Pahang, Malaysia; [b] School of Mathematical Sciences, Faculty of Science and Technology, Universiti Kebangsaan Malaysia, 43600 UKM Bangi,Selangor, Malaysia; [c] Department of Mathematics, Babeș-Bolyai University, 400084 Cluj-Napoca, Romania; [d] Department of Computational and Theoretical Sciences, Kulliyyah of Science, International Islamic University Malaysia, Bandar Indera Mahkota, 25200 Kuantan, Pahang, Malaysia; [e] Faculty of Computer and Mathematical Sciences, Universiti Teknologi MARA, 40450 UiTM Shah Alam, Selangor, Malaysia

Abstract The present study investigates the mathematical model of free convection boundary layer flow from a vertical truncated cone immersed in *Cu*/water nanofluid and *Al₂O₃-Cu*/water hybrid nanofluid. The governing non-linear equations are first transformed to a more convenient set of partial differential equations before being solved numerically using the Keller-box method. The numerical values for the reduced Nusselt number and the reduced skin friction coefficient are obtained and illustrated graphically as well as temperature profiles and velocity profiles. Effects of the alumina *Al₂O₃* and copper *Cu* nanoparticle volume fraction for hybrid nanofluid are analyzed and discussed. It is found that the high-density and highly thermal conductivity nanoparticles like copper contributed more in skin friction and convective heat transfer capabilities. The appropriate nanoparticles combination in hybrid nanofluid may reduce the friction between fluid and surface but yet still gave the heat transfer capabilities comparable to metal nanofluid.

Keywords: Free convection, full-cone, hybrid nanofluid, truncated cone.

Introduction

Recent engineering applications saw the thirst use of nanofluid as a heat transfer medium for example as radiator coolant, tyre production, brake fluid, liquid submerged cooling as well as in electrical devices [1]. Nanofluid has better performance in thermal conductivity, viscosity, thermal diffusivity and convective heat transfer compared to based fluids like water and oil. A study has found that the 5% *CuO*/water nanofluid has a 60% of thermal conductivity higher compared to base fluid [2-4]. Highly performance demand for heat transfer capabilities has pushed the seek for better heat transfer medium along with nanofluid.

Metal nanoparticles like copper *Cu* and silver *Ag* are known to have better performance in heat transfer compared to oxide nanoparticles, thanks to the metal nanoparticle's higher thermal conductivity. Unfortunately, the metal nanomaterial is expensive, dense and not economical in mass production as well as contributed to high fluid-surface friction. The hybrid nanofluid is introduced to blend the gap

between the price and the performance of the nanofluid [5].

Considering the convective flow on a circular cone, these applications are found in many industrial and engineering devices such as the solder tip, the conical heater as well as the secondary pulley in continuous variable transmission (CVT) in a modern car. The continuous changing in gear ratio in CVT needs low friction and efficiency in heat transfer between the V-belt and the pulley. This required an excellent lubricant specifically blended from the nanofluid with low dense particle but high thermal conductivity.

Many investigations regarding the heat transfer towards cone have been done in the past decade, pioneered by Na and Chiou [6-7] who consider the laminar natural convection over a slender horizontal and vertical frustum of a cone. The numerical values for surface temperature for various Prandtl number from a truncated cone to full-cone is analyzed. It is concluded that the surface temperature decreases as the Prandtl number increases. Kumari et al. [8] then consider the mixed convection boundary layer flow. Pop and Na [9] then enriched this study with wavy cone. The analysis on circular cone then have been extended with magnetic effect, radiation effects, pressure work effect, suction/blowing effect [10-12] as well as investigation embedded in nanofluid by Ahmed and Mahdy [13], Chamkha et al. [14], Pătrulescu et al. [15] and Mahdy [16].

Recent studies on fluid flow included the works by Khan et al. [17-18] and Ellahi et al. [19] who investigated the nanofluid containing gyrotactic microorganisms and micropolar nanofluid, respectively while Rao et al. [20] observed the natural convection of carbon nanotubes–water nanofluid flow inside a vertical truncated wavy cone.

Motivated by the above literature, the present study investigates numerically the free convection boundary layer flow and heat transfer from a vertical truncated cone in a hybrid nanofluid. The approach from a numerical analysis is are considers cheap, fast and provided the theoretical knowledge for the hybrid nanofluid, therefore proposing an early idea about the fluid flow and heat transfer characteristics. The study of free convection of hybrid nanofluid on a vertical truncated cone so far is never been done before, so the reported results in this study are new.
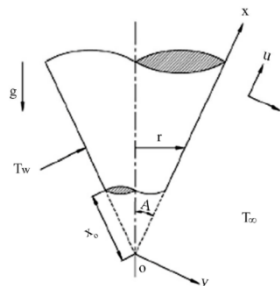
Figure 1. Physical model of the coordinate system.

Mathematical Formulations

Consider a steady, two-dimensional free convection flow and heat transfer of a hybrid nanofluid about an impermeable truncated cone, as shown in Figure 1, where *x* and *y* are the Cartesian coordinate with the x- axis measured along the surface of the cone from the origin, and y- axis is the coordinate normal to the surface of the cone and r is the radius of the truncated cone. The origin of the coordinate system is placed at the vertex of the full cone, where $\bar{x} = x - x_o$ and the constant surface temperature is T_w while the temperature of the ambient fluid is T_∞. It is assumed that the boundary layer develops at the leading edge of the truncated cone $(x = x_o)$. By employing the usual boundary layer approximations, the governing equations of the hybrid nanofluid for the continuity, momentum and energy are written as [5,13]:

$$\frac{\partial(ru)}{\partial x} + \frac{\partial(rv)}{\partial y} = 0, \tag{1}$$

$$u\frac{\partial u}{\partial x} + v\frac{\partial u}{\partial y} = v_{hnf}\frac{\partial^2 u}{\partial y^2} + \frac{(\rho\beta)_{hnf}}{\rho_{hnf}}g(T - T_\infty)\cos A, \tag{2}$$

$$u\frac{\partial T}{\partial x} + v\frac{\partial T}{\partial y} = \frac{k_{hnf}}{(\rho C_p)_{hnf}}\frac{\partial^2 T}{\partial y^2}, \tag{3}$$

subject to the boundary conditions

$$u = v = 0, \; T = T_w \; \text{at} \; y = 0,$$
$$u \to 0, \; T \to T_\infty \; \text{as} \; y \to \infty. \tag{4}$$

where u and v are the velocity components of the hybrid nanofluid along x- and y- axes, T represents the hybrid nanofluid temperature in the boundary layer, g is the gravitation acceleration, A is the half angle of the full cone, $v_{hnf}, \mu_{hnf}, \rho_{hnf}, (\rho C_p)_{hnf}, \beta_{hnf}$ and k_{hnf} represent the kinematic viscosity, dynamic viscosity, density, heat capacity, thermal expansion and thermal conductivity of the hybrid nanofluid, which are given in equation (5) as in Devi and Devi [5]. Further, ϕ_1 and ϕ_2 represent the volume fractions of *Al₂O₃* and *Cu* nanoparticles, respectively where $\phi_1 = \phi_2 = 0$ indicate the regular fluid. Other properties related to base fluid and the nanoparticles are denoted with subscript f and $s1, s2$.

$$v_{hnf} = \frac{\mu_{hnf}}{\rho_{hnf}}, \; \mu_{hnf} = \frac{\mu_f}{(1-\phi_1)^{2.5}(1-\phi_2)^{2.5}},$$

$$\rho_{hnf} = (1-\phi_2)\left[(1-\phi_1)\rho_f + \phi_1\rho_{s1}\right] + \phi_2\rho_{s2},$$

$$(\rho\beta)_{hnf} = (1-\phi_2)\left[(1-\phi_1)(\rho\beta)_f + \phi_1(\rho\beta)_{s1}\right] + \phi_2(\rho\beta)_{s2},$$

$$(\rho C_p)_{hnf} = (1-\phi_2)\left[(1-\phi_1)(\rho C_p)_f + \phi_1(\rho C_p)_{s1}\right] + \phi_2(\rho C_p)_{s2},$$

$$\frac{k_{hnf}}{k_{bf}} = \frac{k_{s2} + 2k_{bf} - 2\phi_2(k_{bf} - k_{s2})}{k_{s2} + 2k_{bf} + \phi_2(k_{bf} - k_{s2})}, \quad \frac{k_{bf}}{k_f} = \frac{k_{s1} + 2k_f - 2\phi_1(k_f - k_{s1})}{k_{s1} + 2k_f + \phi_1(k_f - k_{s1})}.$$

In this study, initially 0.06 vol. solid nanoparticle of $Cu \, (\phi_2 = 0.06)$ is added into water based-fluid to form *Cu*/water nanofluid. Next, 0.1 vol. solid nanoparticle of $Al_2O_3 \, (\phi_1 = 0.1)$ is added into *Cu*/water nanofluid to form the *Al₂O₃-Cu*/water hybrid nanofluid namely. The governing equation and boundary conditions are in dimensional form, thus need to non-dimensionalised before being solved. It is introduced the non-dimensional variable η and ξ and temperature θ are defined as [6-7]:

$$\xi = \frac{\bar{x}}{x_o} = \frac{x - x_o}{x_o}, \quad \eta = \frac{y}{\bar{x}}Gr^{1/4}, \; f(\xi,\eta) = \frac{\psi}{rvGr^{1/4}}, \; \theta(\xi,\eta) = \frac{T - T_\infty}{T_w - T_\infty} \tag{5}$$

with $Gr = \frac{g\beta(T_w - T_\infty)\bar{x}^3}{v^2}$ is a Grashof number while ψ taken as a stream function which satisfies equation (1) such that $ru = \frac{\partial\psi}{\partial y}$ and $rv = -\frac{\partial\psi}{\partial x}$, thus

$$u = \frac{vGr^{1/2}}{\bar{x}}\frac{\partial f}{\partial\eta}, \quad v = -\frac{vGr^{1/4}}{\bar{x}}\left\{\left(\frac{\xi}{1+\xi} + \frac{3}{4}\right)f + \xi\frac{\partial f}{\partial\xi} - \frac{1}{4}\eta f'\right\} \tag{6}$$

where $'$ denotes the differentiation with respect to η. Employing the variables (5), equations (2) and (3) are transformed to the following partial differential equations differential equations:

$$\frac{v_{hnf}}{v_f}f''' + \left(\frac{3}{4} + \frac{\xi}{1+\xi}\right)ff'' - \frac{1}{2}f'^2 + \frac{(\rho\beta)_{hnf}}{\rho_{hnf}\beta_f}\theta = \xi\left[f'\frac{\partial f'}{\partial\xi} - f''\frac{\partial f}{\partial\xi}\right], \tag{7}$$

$$\frac{k_{hnf}/k_f}{(\rho C_p)_{hnf}/(\rho C_p)_f}\frac{1}{\mathrm{Pr}}\theta'' + \left(\frac{3}{4} + \frac{\xi}{1+\xi}\right)f\theta' = \xi\left[f'\frac{\partial\theta}{\partial\xi} - \theta'\frac{\partial f}{\partial\xi}\right], \tag{8}$$

where $\mathrm{Pr} = \dfrac{v_f(\rho C_p)_f}{k_f}$ is a Prandtl number. The hybrid nanofluid expressions are detailed as follows:

$$\frac{v_{hnf}}{v_f} = \frac{1}{(1-\phi_1)^{2.5}(1-\phi_2)^{2.5}\left[(1-\phi_2) + \left[(1-\phi_1) + \phi_1(\rho_{s1}/\rho_f)\right] + \phi_2(\rho_{s2}/\rho_f)\right]},$$

$$\frac{(\rho\beta)_{hnf}}{\rho_{hnf}\beta_f} = \frac{(1-\phi_2)\left[(1-\phi_1)\rho_f + \phi_1(\rho\beta)_{s1}/\beta_f\right] + \phi_2(\rho\beta)_{s2}/\beta_f}{(1-\phi_2)\left[(1-\phi_1)\rho_f + \phi_1\rho_{s1}\right] + \phi_2\rho_{s2}},$$

$$\frac{k_{hnf}(\rho C_p)_f}{k_f(\rho C_p)_{hnf}} = \frac{k_{hnf}/k_f}{(1-\phi_2)\left[(1-\phi_1) + \phi_1(\rho C_p)_{s1}/(\rho C_p)_f\right] + \phi_2(\rho C_p)_{s2}/(\rho C_p)_f},$$

$$\frac{\rho_{hnf}(C_p)_f}{(\rho C_p)_{hnf}} = \frac{(1-\phi_2)\left[(1-\phi_1)\rho_f + \phi_1\rho_{s1}\right] + \phi_2\rho_{s2}}{(1-\phi_2)\left[(1-\phi_1)\rho_f + \phi_1(\rho C_p)_{s1}/(C_p)_f\right] + \phi_2(\rho C_p)_{s2}/(C_p)_f}.$$

The boundary conditions become:

$$f(0,\xi) = 0, \ \frac{\partial f}{\partial\eta}(0,\xi) = 0, \ \theta(0,\xi) = 1,$$

$$\frac{\partial f}{\partial\eta}(\eta,\xi) \to 0, \ \theta(\eta,\xi) \to 0, \ \text{as } \eta \to \infty. \tag{9}$$

Noticed that if $\xi = 0$ (truncated cone), equations (7) and (8) reduce to the following ordinary (similarity) differential equations

$$\frac{v_{hnf}}{v_f}f''' + \frac{3}{4}ff'' - \frac{1}{2}f'^2 + \frac{\beta_{hnf}}{\beta_f}\theta = 0, \tag{10}$$

$$\frac{k_{hnf}/k_f}{(\rho C_p)_{hnf}/(\rho C_p)_f}\frac{1}{\mathrm{Pr}}\theta'' + \frac{3}{4}f\theta' = 0, \tag{11}$$

while for $\xi \to \infty$ (full cone), we have

$$\frac{v_{hnf}}{v_f}f''' + \frac{7}{4}ff'' - \frac{1}{2}f'^2 + \frac{\beta_{hnf}}{\beta_f}\theta = 0, \tag{12}$$

$$\frac{k_{hnf}/k_f}{(\rho C_p)_{hnf}/(\rho C_p)_f}\frac{1}{\mathrm{Pr}}\theta'' + \frac{7}{4}f\theta' = 0. \tag{13}$$

Both the system of equations (10,11) and (12,13) are subjected to the boundary conditions

$$f(0) = f'(0) = 0, \ \theta(0) = 1,$$

$$f'(\eta) \to 0, \ \theta(\eta) \to 0, \ \text{as } \eta \to \infty. \tag{14}$$

The physical quantities of interest are the skin friction coefficient C_f and the local Nusselt number Nu_x which given by

$$C_f = \frac{2\tau_w}{\rho_f u_r^2}, \quad Nu_x = \frac{xq_w}{k_f(T_w - T_\infty)}. \tag{15}$$

The surface shear stress τ_w and the surface heat flux q_w are given by

$$\tau_w = \mu_{hnf}\left(\frac{\partial u}{\partial y}\right)_{y=0}, \qquad q_w = -k_{hnf}\left(\frac{\partial T}{\partial y}\right)_{y=0}. \tag{16}$$

Using variables in equations (5) and (16) give

$$C_f Gr^{1/4} = \left(\frac{2}{(1-\varphi)^{2.5}}\right) f''(\xi,0) \text{ and } Nu_x Gr^{-1/4} = -\left(\frac{k_{nf}}{k_f}\right)\theta'(\xi,0). \tag{17}$$

Numerical Method

The partial differential equations (7) and (8) subject to boundary conditions (9) are solved numerically using the Keller-box method. The algorithm of the Keller-box method is coded into MATLAB software to numerically compute. Proposed by Keller [21], this method is an implicit finite difference method with Newton's method for linearization, thus make it suitable for solving non-linear equations at any order. This method have been clearly described by Na [22], Cebeci and Cousteix [23] and recently by Mohamed [24].

Finite Difference Scheme
Keller-box method starts with reducing the equations (7) and (8) with boundary conditions (9) to a first-order system. This is done by introducing the new dependent variables $u(\eta,\xi)$, $v(\eta,\xi)$, $t(\eta,\xi)$ and $\theta = s(\eta,\xi)$ so that $f' = u$, $u' = v$, $s' = t$. The equations (7) and (8) can be written as

$$\frac{v_{hnf}}{v_f}v' + \left(\frac{3}{4} + \frac{\xi}{1+\xi}\right)fv - \frac{1}{2}u^2 + \frac{(\rho\beta)_{hnf}}{\rho_{hnf}\beta_f}s = \left[u\frac{\partial u}{\partial\xi} - v\frac{\partial f}{\partial\xi}\right], \tag{18}$$

$$\frac{k_{hnf}/k_f}{(\rho C_p)_{hnf}/(\rho C_p)_f}\frac{1}{\Pr}t' + \left(\frac{3}{4} + \frac{\xi}{1+\xi}\right)ft = \xi\left[u\frac{\partial s}{\partial\xi} - t\frac{\partial f}{\partial\xi}\right], \tag{19}$$

Next, the net rectangle in the $\eta-$ and $\xi-$ plane are considered and the net points defined as

$$\eta_0 = 0, \qquad \eta_j = \eta_{j-1} + h_j, \qquad j = 1,2,...,J,$$
$$\xi^0 = 0, \qquad \xi^n = \xi^{n-1} + k_n, \qquad n = 1,2,...,N, \tag{20}$$

where $h_j = \Delta\eta_j$ and $k_n = \Delta\xi_n$. Here n and j are the sequence of numbers that indicate the coordinate location, not tensor indices or exponents. The finite difference forms for any points are

$$(\ )_{j-1/2}^n = \frac{1}{2}\left[(\ )_j^n + (\ )_{j-1}^n\right], \tag{21}$$

$$\left(\frac{\partial u}{\partial\eta}\right)_{j-1/2}^{n-1/2} = \frac{u_j^{n-1/2} - u_{j-1}^{n-1/2}}{h_j} \tag{22}$$

The approximate of finite difference for equations (18) and (19) are written by considering the mid-point $\left(\eta_{j-1/2}, \xi^n\right)$ by using the central differences. Hence, the following are obtained:

$$\frac{f_j^n - f_{j-1}^n}{h_j} = \frac{u_j^n + u_{j-1}^n}{2} = u_{j-1/2}^n, \tag{23}$$

$$\frac{u_j^n - u_{j-1}^n}{h_j} = \frac{v_j^n + v_{j-1}^n}{2} = v_{j-1/2}^n, \tag{24}$$

$$\frac{s_j^n - s_{j-1}^n}{h_j} = \frac{t_j^n + t_{j-1}^n}{2} = t_{j-1/2}^n, \tag{25}$$

while the finite centered differential equation at $(\eta_{j-1/2}, \xi^{n-1/2})$ can be denoted as L_1 and L_2 respectively then, the finite difference equations (18) – (19) become

$$\frac{1}{2}\left(L_1^n + L_1^{n-1}\right) = \xi^{n-1/2}\left[u^{n-1/2}\frac{u^n - u^{n-1}}{k_n} - v^{n-1/2}\frac{f^n - f^{n-1}}{k_n}\right], \tag{26}$$

$$\frac{1}{2}\left(L_2^n + L_2^{n-1}\right) = \xi^{n-1/2}\left[u^{n-1/2}\frac{s^n - s^{n-1}}{k_n} - t^{n-1/2}\frac{f^n - f^{n-1}}{k_n}\right], \tag{27}$$

Considering the boundary conditions (19), it can be written as

$$f(0,\xi) = 0, \ u(0,\xi) = 0, \ s(0,\xi) = 1, \ u(\infty,\xi) \to 0, \ s(\infty,\xi) \to 0, \tag{28}$$

At $x = x^{n,}$ the boundary conditions (28) is simplified as

$$f_0^n = 0, \ u_0^n = 0, \ s_0^n = 1, \ u_J^n = 0, \ s_J^n = 0. \tag{29}$$

Newtons Method

Newton's method is used to solve these nonlinear equations (23)-(27). Hence, the following iterates are introduced

$$f_j^{(k+1)} = f_j^{(k)} + \delta f_j^{(k)}, \quad u_j^{(k+1)} = u_j^{(k)} + \delta u_j^{(k)}, \quad v_j^{(k+1)} = v_j^{(k)} + \delta v_j^{(k)},$$
$$s_j^{(k+1)} = s_j^{(k)} + \delta s_j^{(k)}, \quad t_j^{(k+1)} = t_j^{(k)} + \delta t_j^{(k)} \tag{30}$$

Substituting these expressions into equations (23)-(27) and then drop the quadratic and higher-order terms in $\delta f_j^{(k)}$, $\delta u_j^{(k)}$, $\delta v_j^{(k)}$, $\delta s_j^{(k)}$ and $\delta t_j^{(k)}$, this procedure yields the following linear tridiagonal system (dropped the superscript (*k*) for simplicity):

$$\delta f_j - \delta f_{j-1} - \frac{1}{2}h_j\left(\delta u_j + \delta u_{j-1}\right) = (r_1)_{j-1/2}$$

$$\delta u_j - \delta u_{j-1} - \frac{1}{2}h_j\left(\delta v_j + \delta v_{j-1}\right) = (r_2)_{j-1/2}$$

$$\delta s_j - \delta s_{j-1} - \frac{1}{2}h_j\left(\delta t_j + \delta t_{j-1}\right) = (r_3)_{j-1/2}$$

$$(a_1)_j \, \delta v_j + (a_2)_j \, \delta v_{j-1} + (a_3)_j \, \delta f_j + (a_4)_j \, \delta f_{j-1}$$
$$+ (a_5)_j \, \delta u_j + (a_6)_j \, \delta u_{j-1} + (a_7)_j \, \delta s_j + (a_8)_j \, \delta s_{j-1} = (r_4)_{j-1/2},$$

$$(b_1)_j \, \delta t_j + (b_2)_j \, \delta t_{j-1} + (b_3)_j \, \delta f_j + (b_4)_j \, \delta f_{j-1} + (b_5)_j \, \delta s_j +$$
$$(b_6)_j \, \delta s_{j-1} + (b_7)_j \, \delta u_j + (b_8)_j \, \delta u_{j-1} + (b_9)_j \, \delta v_j + (b_{10})_j \, \delta v_{j-1} = (r_5)_{j-1/2}, \tag{31}$$

where

$$(a_1)_j = \frac{v_{hnf}}{v_f} + \frac{h_j(m+\alpha)}{2}f_{j-1/2} - \frac{h_j\alpha}{2}f_{j-1/2}^{n-1}, \quad (a_2)_j = (a_1)_j - 2\frac{v_{hnf}}{v_f},$$

$$(a_3)_j = (a_4)_j = \frac{h_j(m+\alpha)}{2}v_{j-1/2} + \frac{h_j\alpha}{2}v_{j-1/2}^{n-1},$$

$$(a_5)_j = (a_6)_j = -h_j(0.5+\alpha)u_{j-1/2},$$ (32)

$$(a_7)_j = (a_8)_j = \frac{(\rho\beta)_{hnf}}{\rho_{hnf}\beta_f}\frac{h_j}{2},$$

$$(b_1)_j = \frac{k_{hnf}(\rho C_p)_f}{k_f(\rho C_p)_{hnf}}\frac{1}{\Pr} + \frac{h_j(m+\alpha)}{2}f_{j-1/2} - \frac{h_j\alpha}{2}f_{j-1/2}^{n-1},$$

$$(b_2)_j = (b_1)_j - \frac{2}{\Pr}\frac{k_{hnf}(\rho C_p)_f}{k_f(\rho C_p)_{hnf}},$$

$$(b_3)_j = (b_4)_j = \frac{h_j(m+\alpha)}{2}t_{j-1/2} + \frac{h_j\alpha}{2}t_{j-1/2}^{n-1},$$ (33)

$$(b_5)_j = (b_6)_j = -\frac{h_j\alpha}{2}u_{j-1/2} - \frac{h_j\alpha}{2}u_{j-1/2}^{n-1},$$

$$(b_7)_j = (b_8)_j = -\frac{h_j\alpha}{2}s_{j-1/2} + \frac{h_j\alpha}{2}s_{j-1/2}^{n-1},$$

and

$$(r_1)_{j-1/2} = f_{j-1} - f_j + h_j u_{j-1/2},$$

$$(r_2)_{j-1/2} = u_{j-1} - u_j + h_j v_{j-1/2},$$

$$(r_3)_{j-1/2} = s_{j-1} - s_j + h_j t_{j-1/2},$$ (34)

$$(r_4)_{j-1/2} = \frac{v_{hnf}}{v_f}(-v_j + v_{j-1}) - h_j\left[(m+\alpha)f_{j-1/2}v_{j-1/2} - ...\right] + (R_1)_{j-1/2},$$

$$(r_5)_{j-1/2} = \frac{k_{hnf}(\rho C_p)_f}{k_f(\rho C_p)_{hnf}}\frac{1}{\Pr}(-t_j + t_{j-1}) - h_j\left[(m+\alpha)f_{j-1/2}t_{j-1/2} + ...\right] + (R_2)_{j-1/2}$$

Recall the boundary conditions (29), which can be satisfied exactly with no iteration. Therefore, in order to maintain these correct values in all the iterates,

$$\delta f_0 = 0, \; \delta u_0 = 0, \; \delta s_0 = 0, \; , \delta u_J = 0 \text{ and } \delta s_J = 0.$$ (35)

The Block Elimination Technique
Usually, the three diagonal block structure consists of variable or constants, but here in Keller-box method is different because it consists of block matrices. The elements of the matrices are defined as follows:

$$
\begin{bmatrix}
[A_1] & [C_1] & & & & & \\
[B_2] & [A_2] & [C_2] & & & & \\
& & \ddots & & & & \\
& & & \ddots & & & \\
& & & & \ddots & & \\
& & & & [B_{J-1}] & [A_{J-1}] & [C_{J-1}] \\
& & & & & [B_J] & [A_J]
\end{bmatrix}
\begin{bmatrix}
[\delta_1] \\
[\delta_2] \\
\vdots \\
[\delta_{J-1}] \\
[\delta_J]
\end{bmatrix}
=
\begin{bmatrix}
[r_1] \\
[r_2] \\
\vdots \\
[r_{J-1}] \\
[r_J]
\end{bmatrix}
$$

That is

$$
[A][\delta] = [r] \tag{20}
$$

where

$$
[A_1] = \begin{bmatrix}
0 & 0 & 1 & 0 & 0 \\
d & 0 & 0 & d & 0 \\
0 & d & 0 & 0 & d \\
a_2 & 0 & a_3 & a_1 & 0 \\
0 & b_2 & b_3 & 0 & b_1
\end{bmatrix} \quad d = -\frac{h_1}{2},
$$

$$
[A_j] = \begin{bmatrix}
d & 0 & 1 & 0 & 0 \\
-1 & 0 & 0 & d & 0 \\
0 & -1 & 0 & 0 & d \\
a_6 & a_8 & a_3 & a_1 & 0 \\
b_8 & b_6 & b_3 & 0 & b_1
\end{bmatrix} \quad d = -\frac{h_j}{2}, 2 \le j \le J,
$$

$$
[B_j] = \begin{bmatrix}
0 & 0 & -1 & 0 & 0 \\
0 & 0 & 0 & d & 0 \\
0 & 0 & 0 & 0 & d \\
0 & 0 & a_4 & a_2 & 0 \\
0 & 0 & b_4 & 0 & b_2
\end{bmatrix}, d = -\frac{h_j}{2}, 2 \le j \le J
$$

$$
[C_j] = \begin{bmatrix}
d & 0 & 0 & 0 & 0 \\
1 & 0 & 0 & 0 & 0 \\
0 & 1 & 0 & 0 & 0 \\
a_5 & a_7 & 0 & 0 & 0 \\
b_7 & b_5 & 0 & 0 & 0
\end{bmatrix}, d = -\frac{h_j}{2}, 2 \le j \le J \tag{25}
$$

$$
[\delta_1] = \begin{bmatrix}
\delta v_0 \\
\delta t_0 \\
\delta f_1 \\
\delta v_1 \\
\delta t_1
\end{bmatrix}, \quad
[\delta_j] = \begin{bmatrix}
\delta u_{j-1} \\
\delta s_{j-1} \\
\delta f_j \\
\delta v_j \\
\delta t_j
\end{bmatrix}, \quad \text{and } [r_j] = \begin{bmatrix}
(r_1)_{j-1/2} \\
(r_2)_{j-1/2} \\
(r_3)_{j-1/2} \\
(r_4)_{j-1/2} \\
(r_5)_{j-1/2}
\end{bmatrix},
$$

To solve the equation (20), assuming that *A* is nonsingular matrices and it can be factorized as

$$[A]=[L][U] \tag{26}$$

where

$$[L]=\begin{bmatrix} [\alpha_1] & & & & \\ [B_2] & [\alpha_2] & & & \\ & & \ddots & & \\ & & \ddots & [\alpha_{J-1}] & \\ & & & [B_J] & [\alpha_J] \end{bmatrix} \text{ and } [U]=\begin{bmatrix} [I] & [\Gamma_1] & & & \\ & [I] & [\Gamma_2] & & \\ & & \ddots & & \\ & & & \ddots & \\ & & & [I][\Gamma_{J-1}] \\ & & & & [I] \end{bmatrix},$$

$[I]$ is the identity matrix of order 5 and $[\alpha_i]$, and $[\Gamma_i]$ are 5×5 matrices which elements are determined by the following equations:

$$[\alpha_1]=[A_1] \tag{27}$$

$$[A_1][\Gamma_1]=[C_1] \tag{28}$$

and

$$[\alpha_j]=[A_j]-[B_j][\Gamma_{j-1}], \quad j = 2, 3, \ldots, J \tag{29}$$

$$[\alpha_j][\Gamma_j]=[C_j], \quad j = 2, 3, \ldots, J\text{-}1. \tag{30}$$

Equation (26) are substituted into equation (20), thus

$$[L][U][\delta]=[r]. \tag{31}$$

Let

$$[U][\delta]=[W] \tag{32}$$

then equation (31) becomes

$$[L][W]=[r] \tag{33}$$

where

$$W=\begin{bmatrix} [W_1] \\ [W_2] \\ \vdots \\ [W_{J-1}] \\ [W_J] \end{bmatrix}$$

and the $[W_j]$ are the 5×1 column matrices. The elements W can be solved from equation (33) by

$$[\alpha_1][W_1]=[r_1] \tag{34}$$

$$[\alpha_j][W_j]=[r_j]-[B_j][W_{j-1}], \quad 2 \leq j \leq J. \tag{35}$$

The step in which Γ_j, α_j and W_j are calculated is usually referred as the forward sweep. Once the elements of *W* are found, equation (32) then gives the solution δ in the so-called backward sweep, in which the elements are obtained by the following relations:

$$[\delta_J]=[W_J] \tag{36}$$

$$[\delta_j]=[W_j]-[\Gamma_j][\delta_{j+1}], \quad 1 \leq j \leq J-1. \tag{37}$$

These calculations are repeated until some convergence criterion is satisfied and calculations are stopped when

$$\left| \delta v_0^{(i)} \right| < 10^{-6} \tag{38}$$

Results and Discussions

The computation focused on the effects of a pertinent parameter which is the Prandtl number Pr and the nanoparticle volume fraction for alumina $Al_2O_3\,(\phi_1)$ and copper $Cu(\phi_2)$. The calculation is obtained for the truncated cone $(\xi = 0)$ extending to the end of the cone $(\xi = \infty)$. Table 1 shows the values of thermophysical properties of water and nanoparticles considered. For comparison purposes, Table 2 shows the comparison values of heat transfer coefficient for based fluid ($\phi_1 = \phi_2 = 0$) with previously published results. From Table 2, it is found that the results agreed and are in a good agreement, hence it is believed that the whole results present in this study are precise in computing numerically.

Table 1. Thermophysical properties of water and nanoparticles.

Physical Properties	Water (f)	$Al_2O_3\,(\phi_1)$	$Cu(\phi_2)$
ρ (kg/m3)	997	3970	8933
C_p (J/kg·K)	4179	765	385
k(W/m·K)	0.613	40	400
β (1/K)	2.1x10^{-4}	0.85x10^{-5}	1.67x10^{-5}

Table 2. Comparison values of $-\theta'(0)$ with previous published results for various values of Pr when $\phi_1 = \phi_2 = 0$.

Pr	$\xi = 0$ (truncated cone)			$\xi \to \infty$ (full cone)		
	Na and Chiou [6]	Chamkha [11]	Present	Na and Chiou [6]	Chamkha [11]	Present
0.01	0.05742	0.0574	0.0591	0.07493	0.0751	0.0767
0.7	0.35320	-	0.3533	0.45101	-	0.4511
1	0.40110	0.4015	0.4009	0.51039	0.5111	0.5104
7	-	-	0.7455	-	-	0.9342
10	0.82690	0.8274	0.8269	1.03397	1.0342	1.0341
100	1.54930	1.5503	1.5496	1.92197	1.9230	1.9234

Figures 2 and 3 show the variation of the reduced skin friction coefficient $C_f Gr^{1/4}$ and reduced Nusselt number $Nu_x Gr^{-1/4}$ along the non-dimensional streamwise coordinate ξ for various values of ϕ_1 and ϕ_2, respectively. From Figure 2, it was found that values of the $C_f Gr^{1/4}$ is unique for a truncated cone $(\xi = 0)$. As ξ increases, the values of $C_f Gr^{1/4}$ also increase. It is a sign that skin friction increases with the length of the cone. Next, the variation of $C_f Gr^{1/4}$ for *Cu*/water ($\phi_1 = 0.0,\ \phi_2 = 0.06$) nanofluid is higher than water-based fluid ($\phi_1 = 0.0,\ \phi_2 = 0.0$). Adding 0.1 vol. of alumina Al_2O_3 nanoparticles into *Ag*/water nanofluid to form the *Al₂O₃-Ag*/water ($\phi_1 = 0.1,\ \phi_2 = 0.06$) hybrid nanofluid provided more $C_f Gr^{1/4}$. It is noticed that *Cu*/water ($\phi_1 = 0.0,\ \phi_2 = 0.16$) nanofluid provided higher values of $C_f Gr^{1/4}$ compared to all fluids tested. This is realistic because the increase of nanoparticle in fluid increased the friction between fluid and surface. Further, *Cu* has a higher density compared to Al_2O_3 thus contributing to high friction. Practically, the hybrid nanofluid tested shows that the skin friction can be reduced by selecting the appropriate combination of metal and oxide nanoparticles.

Figure 3 shows almost similar trends to Figure 2. It is noticed that the $Nu_x Gr^{-1/4}$ is increasing along ξ. The *Cu*/water ($\phi_1 = 0.0,\ \phi_2 = 0.16$) nanofluid score highest values in $Nu_x Gr^{-1/4}$, followed closely by the *Al₂O₃-Cu*/water ($\phi_1 = 0.1,\ \phi_2 = 0.06$) hybrid nanofluid compared to water-based fluid and *Cu*/water

$(\phi_1 = 0.0, \phi_2 = 0.06$)nanofluid. It is clearly shown that the hybrid nanofluid which consists of a combination of metal and low-cost oxide nanoparticles generate comparable heat transfer capabilities with metal nanofluid.
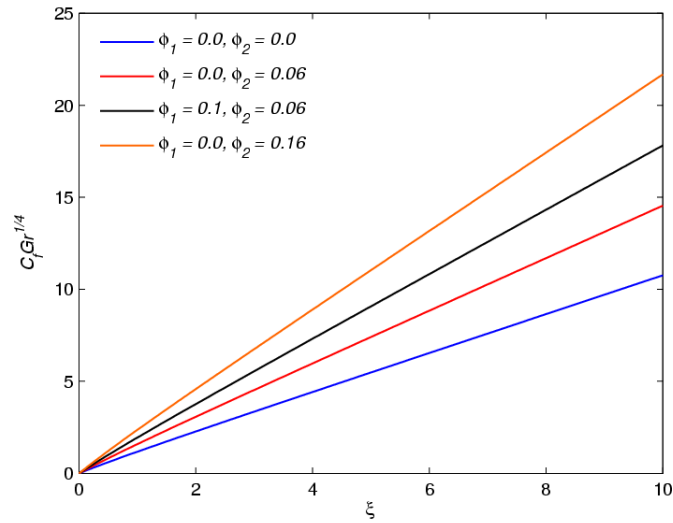
Figure 2: Variation of $C_f Gr^{1/4}$ against ξ for various values of ϕ_1 and ϕ_2 when $\mathrm{Pr} = 7$
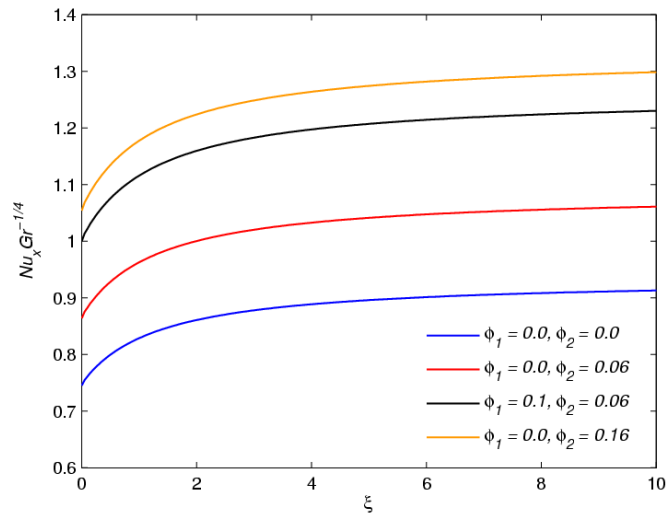
Figure 3: Variation of $Nu_x Gr^{-1/4}$ against ξ for various values of ϕ_1 and ϕ_2 when $\mathrm{Pr} = 7$

The temperature profiles $\theta(\eta)$ and velocity profiles $f'(\eta)$ of a truncated cone $(\xi = 0)$ for various values of ϕ_1 and ϕ_2 are illustrated in Figures 4 and 5, respectively. In Figure 4, it is shown the increase of nanoparticles has increased the thermal boundary layer thickness. The increase of nanoparticles enhanced thermal conductivity in fluid thus raising the thermal diffusivity and increasing the thermal boundary layer thickness. From Figure 5, the increase of nanoparticles enhanced the velocity while reducing the velocity boundary layer thicknesses. The increase in nanoparticles raised the fluid momentum which translates to the increase in fluid velocity. This is not surprising for the nanofluid with denser nanoparticles like copper *Cu* in *Cu*/water $(\phi_1 = 0.0, \phi_2 = 0.16$) nanofluid. The higher density nanofluid or hybrid nanofluid highly decelerates compared to a less dense water-based fluid, thus leading to a reduction in velocity boundary layer thickness.
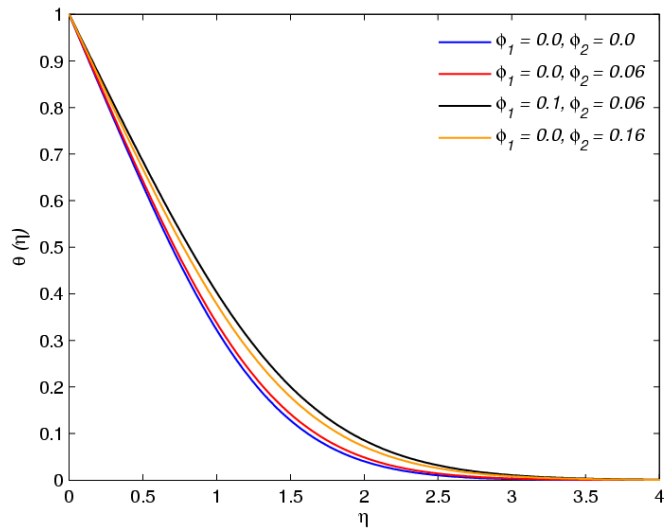
Figure 4: Temperature profiles $\theta(\eta)$ against η for various values of ϕ_1 and ϕ_2 when $\mathrm{Pr} = 7$

Lastly, Figures 6 and 7 illustrate the temperature profiles $\theta(\eta)$ and velocity profiles $f'(\eta)$ for various values of ξ, respectively. Both figures gave information that the thermal and velocity boundary layer thicknesses for the truncated cone $(\xi = 0)$ is greater than the full cone $(\xi = \infty)$. Further, it is observed that the increase of ξ results in the increase in both thermal and velocity boundary layer thicknesses. This situation led to the increase of temperature gradient and velocity gradient, respectively thus supporting the increase in $C_f Gr^{1/4}$ and $Nu_x Gr^{-1/4}$ found in Figures 2 and 3.
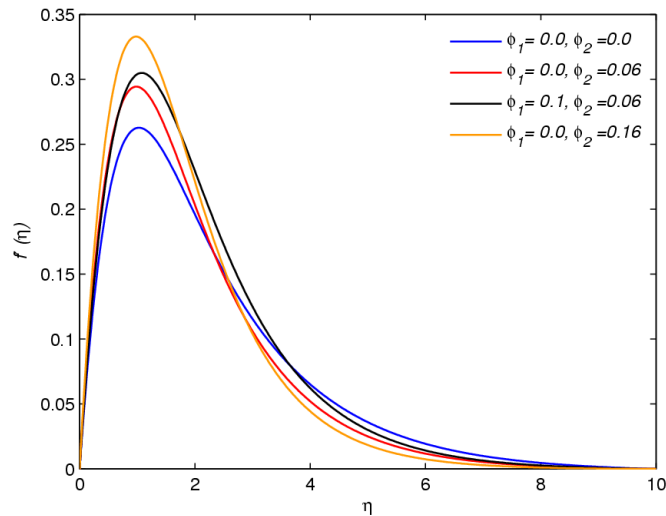
Figure 5: Velocity profiles $f'(\eta)$ against η for various values of ϕ_1 and ϕ_2 when $\mathrm{Pr} = 7$
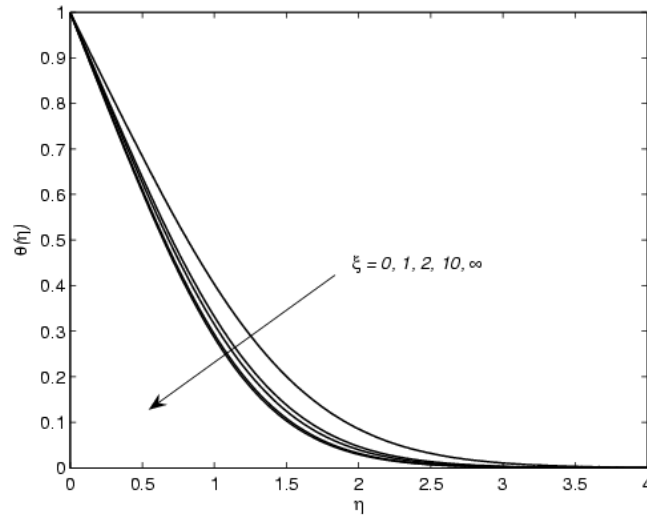
Figure 6: Temperature profiles $\theta(\eta)$ against η for various values of ξ when $\phi_1 = 0.1$ and $\phi_2 = 0.06$
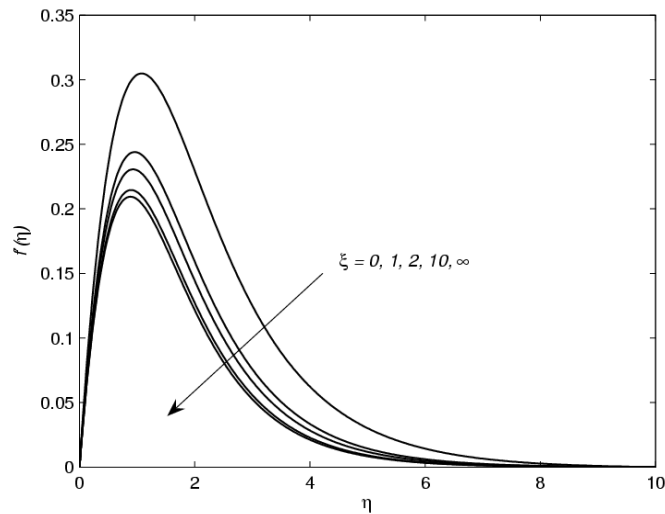
Figure 7: Velocity profiles $f'(\eta)$ against η for various values of ξ when $\phi_1 = 0.1$ and $\phi_2 = 0.06$

Conclusions

The present paper solved numerically the mathematical model of free convection boundary layer flow from a vertical truncated cone embedded in a hybrid nanofluid. The effects of Prandtl number Pr, alumina Al_2O_3 (ϕ_1) and copper Cu (ϕ_2) nanoparticles volume fraction for hybrid nanofluid are analyzed and discussed.

In summary, the increase in streamwise function enhanced both skin friction coefficient and the Nusselt number while the fluid velocity and a thermal boundary layer thickness decreased. This situation clearly indicates that the truncated cone has a lower skin friction coefficient and the Nusselt number compared to a full cone.

Further, it is observed that the increase of nanoparticle volume fraction in the fluid has increased the skin friction coefficient, the Nusselt number, the thermal boundary layer thickness and the fluid velocity. The high-density and highly thermal conductivity nanoparticles like copper contributed more to skin friction and convective heat transfer capabilities. In summary, it is suggested that the appropriate nanoparticles

combination in hybrid nanofluid may reduce the friction between fluid and surface but yet still gave the heat transfer capabilities comparable to metal nanofluid.

Conflicts of Interest

The author(s) declare(s) that there is no conflict of interest regarding the publication of this paper.

Acknowledgment

References

[1]   Wong, K. V. and De Leon, O. (2010). Applications of Nanofluids: Current and Future *Advances in Mechanical Engineering*, 2010 1-11.
[2]   Eastman, J., Choi, U., Li, S., Thompson, L. and Lee, S. 1997. Enhanced thermal conductivity through the development of nanofluids. *Materials Research Society proceedings,* Pittsburgh. Cambridge Univ Press.
[3]   Choi, S. U. S., Zhang, Z. G., Yu, W., Lockwood, F. E. and Grulke, E. A. (2001). Anomalously thermal conductivity enhancement in nanotube suspensions *Applied Physics Letters*, 79 2252-2254.
[4]   Kakaç, S. and Pramuanjaroenkij, A. (2009). Review of convective heat transfer enhancement with nanofluids *International Journal of Heat and Mass Transfer*, 52(13–14), 3187-3196.
[5]   Devi, S. S. U. and Devi, S. P. A. (2017). Heat transfer enhancement of Cu - Al2O3/water hybrid nanofluid flow over a stretching sheet *Journal of the Nigerian Mathematical Society*, 36(2), 419-433.
[6]   Na, T.-Y. and Chiou, J. (1979). Laminar natural convection over a frustum of a cone *Applied Scientific Research*, 35(5-6), 409-421.
[7]   Na, T. and Chiou, J. (1979). Laminar natural convection over a slender vertical frustum of a cone *Wärme-und Stoffübertragung*, 12(2), 83-87.
[8]   Kumari, M., Pop, I. and Nath, G. (1989). Mixed convection along a vertical cone *International Communications in Heat and Mass Transfer*, 16(2), 247-255.
[9]   Pop, I. and Na (1999). Natural convection over a vertical wavy frustum of a cone *International Journal of Non-Linear Mechanics*, 34 925-934.
[10]   Yih, K. (1999). Effect of radiation on natural convection about a truncated cone *International Journal of Heat and Mass Transfer*, 42(23), 4299-4305.
[11]   Chamkha, A. J. (2001). Coupled heat and mass transfer by natural convection about a truncated cone in the presence of magnetic field and radiation effects *Numerical Heat Transfer: Part A: Applications*, 39(5), 511-530.
[12]   Alim, M., Alam, M. M. and Chowdhury, M. M. (2006). Pressure work effect on natural convection flow from a vertical circular cone with suction and non-uniform surface temperature *Journal of Mechanical Engineering*, 36 6-11.
[13]   Ahmed, S. E. and Mahdy, A. (2012). Natural convection flow and heat transfer enhancement of a nanofluid past a truncated cone with magnetic field effect *World Journal of Mechanics*, 2(05), 272-279.
[14]   Chamkha, A., Abbasbandy, S., Rashad, A. M. and Vajravelu, K. (2013). Radiation effects on mixed convection about a cone embedded in a porous medium filled with a nanofluid *Meccanica*, 48(2), 275-285.
[15]   Pătrulescu, F., Groşan, T. and Pop, I. (2014). Mixed convection boundary layer flow from a vertical truncated cone in a nanofluid *International Journal of Numerical Methods for Heat & Fluid Flow*, 24 1175-1190.
[16]   Mahdy, A. (2016). Natural convection boundary layer flow due to gyrotactic microorganisms about a vertical cone in porous media saturated by a nanofluid *Journal of the Brazilian Society of Mechanical Sciences and Engineering*, 38(1), 67-76.
[17]   Khan, W. A., Rashad, A., Abdou, M. and Tlili, I. (2019). Natural bioconvection flow of a nanofluid containing gyrotactic microorganisms about a truncated cone *European Journal of Mechanics-B/Fluids*, 75 133-142.
[18]   Khan, W. A., Rashad, A., EL-Kabeir, S. and EL-Hakiem, A. (2020). Framing the MHD Micropolar-Nanofluid Flow in Natural Convection Heat Transfer over a Radiative Truncated Cone *Processes*, 8(4), 379.
[19]   Ellahi, R., Zeeshan, A., Waheed, A., Shehzad, N. and Sait, S. M. (2021). Natural convection nanofluid flow with heat transfer analysis of carbon nanotubes–water nanofluid inside a vertical truncated wavy cone *Mathematical Methods in the Applied Sciences*, 202 11-19.
[20]   Rao, M. V. S., Gangadhar, K., Chamkha, A. J. and Surekha, P. (2021). Bioconvection in a Convectional Nanofluid Flow Containing Gyrotactic Microorganisms over an Isothermal Vertical Cone Embedded in a Porous Surface with Chemical Reactive Species *Arabian Journal for Science and Engineering*, 46(3), 2493-2503.
[21]   Keller, H. B. (1970). A New Difference Scheme for Parabolic Problems. Dalam: Bramble, Numerical Solutions of Partial Differential Equations. New York: Academic Press 1970.
[22]   Na, T. Y. (1979). Computational methods in engineering boundary value problems. New York: Academic Press 1979.
[23]   Cebeci, T. and Cousteix, J. (2005). Modeling and computation of boundary layer flows. Springer 2005.
[24]   Mohamed, M. K. A. (2018). Keller-box method: Partial differential equations in boundary layer flow of nanofluid. Pekan: DRB-HICOM University Publisher 2018.